Article:
Oh, J.X., Mackie, A.R., Ettelaie, R. et al. (2 more authors) (2025) Bioaccessibility and Absorption of Curcumin: A Look into γ-Cyclodextrin Metal-Organic Frameworks. Chemical Engineering and Process Techniques, 10 (2). 1104. ISSN: 2333-6633

SciMedCentral

Chemical Engineering & Process Techniques

Research Article

Bioaccessibility and Absorption of Curcumin: A Look into γ-Cyclodextrin Metal-Organic Frameworks

Jia X. Oh, Alan R. Mackie, Rammile Ettelaie, Taskeen Niaz, and Brent S. Murray*

Food Colloids and Bioprocessing Group, School of Food Science and Nutrition, University of Leeds, UK

***Corresponding author**

Brent S. Murray, Food Colloids and Bioprocessing Group, University of Leeds, Leeds, LS2 9JT, UK, Tel: 44 (0)113 34 32962

Submitted: 31 July, 2025

Accepted: 09 September, 2025

Published: 10 September, 2025

ISSN: 2333-6633

Keywords

• Curcumin; γ-Cyclodextrin Metal-Organic Frameworks; Encapsulation; Bioaccessibility; Absorption

Abstract

Curcumin has long been recognized for its potential pharmacological effects. However, its bioaccessibility and bioavailability remain low. To address this limitation, we evaluated the efficiency of delivery via curcumin-encapsulated γ-cyclodextrin metal-organic frameworks (Cur-γ-CD-MOFs), in comparison to coarse emulsions formulated with sodium caseinate and Tween 80, using simulated *in vitro* gastrointestinal digestion. Bioaccessibility of curcumin was highest when encapsulated in γ-CD-MOFs, if delivered as a capsule to avoid exposure to gastric conditions, achieving a sixfold increase compared to native (non-encapsulated) curcumin and significantly higher than the emulsion systems if exposed to gastric conditions (due to the structural instability of γ-CD-MOFs under acidic gastric conditions). It was also demonstrated that, prolonged solubilization of curcumin via capsule-delivered γ-CD-MOFs throughout *in vitro* gastrointestinal digestion enhanced its transport and absorption across the mouse intestinal epithelial tissue. This highlights the potential of γ-CD-MOFs as an effective delivery system for improving bioaccessibility and absorption of bioactive compounds.

Highlights

Cur-γ-CD-MOFs delivered as a capsule enhance curcumin bioaccessibility

Cur-γ-CD-MOFs degrade in emulsions under gastric (acid) conditions

Ex vivo Using chamber validates improved intestinal absorption via CD-MOFs

INTRODUCTION

Curcumin, derived from the root of Curcuma longa (turmeric), is a mixture of three principal compounds – curcumin, demethoxycurcumin and bisdemethoxycurcumin – collectively referred to as curcuminoids [1,2]. Due to their physiologically active functionality as a natural antioxidant contributing to the prevention of multiple diseases, curcuminoids have garnered a lot of attention throughout the past decade [3]. Curcumin's bioavailability is limited due to poor absorption, significant liver metabolism, and excretion via the gall bladder. It is also pH-sensitive and becomes increasingly more unstable in basic pH (> pH 7). Therefore, to enhance its therapeutic effects and practical applications, various encapsulation techniques – such as liposomes, nanoparticles, emulsions, gels, cyclodextrin inclusion complexes – have been developed, demonstrating improved stability and controlled delivery of curcumin [4,5].

γ-Cyclodextrin metal-organic frameworks (γ-CD-MOFs) are porous, versatile, crystalline materials composed of γ-cyclodextrin (γ-CD) units linked by metal ions, such as potassium or other alkaline metals. The γ-CD-MOFs preserve the γ-CD hydrophobic central cavity and outer hydrophilic surface and so provide excellent biocompatibility and enhanced solubility and stability of various less polar bioactive compounds encapsulated within them [6]. Following a detailed characterization study [7], confirming their structural integrity, curcumin was thought to be encapsulated not only within the hydrophobic cavities (via van der Waals forces and hydrophobic interactions), but also between γ-CD pairs in the crystallites, via hydrogen bonding between hydroxyl groups. Further analysis [8], also showed that micelles could take up curcumin prematurely released from the cavities of the γ-CD-MOFs as they dissociated in an aqueous environment, leading to further enhanced apparent solubility and bioaccessibility of curcumin. Therefore,

supplementing the γ-CD-MOF encapsulation system within an appropriate surfactant-rich system, such as an oil-in-water (O/W) emulsion, may further boost the fraction of curcumin that would be potentially bioavailable.

Emulsions are widely used for delivering bioactives, potentially protecting hydrophobic compounds from degradation and allowing their controlled release, though the emulsion stability and release will depend on the chosen emulsifier. Sodium caseinate (NaCas) is a natural composite mixture of milk proteins that generally imparts excellent stabilization of O/W emulsions via electrostatic and steric repulsion at the O-W interface[9,10].Tween 80, a synthetic non-ionic surfactant, is also an efficient emulsifier [11]. These two very different types of emulsifiers, digestible and non-digestible, were therefore chosen for comparison in the first direct assessment of curcumin bioaccessibility via Cur-γ-CD-MOFs, with and without O/W emulsions, when subjected to simulated gastrointestinal conditions. In addition, this is the first study to evaluate encapsulated curcumin absorption in an *ex vivo* intestinal transport model, in this case via an Ussing chamber. The findings provide valuable insights into the potential of γ-CD-MOFs to enhance curcumin bioaccessibility and absorption.

MATERIALS AND METHODS

Materials

Curcumin (from Curcuma longa (turmeric), powder, >65% purity), γ-cyclodextrin (γ-CD, >90% purity), sodium caseinate (NaCas), D-glucose, mannitol, Nile Red (technical grade) and dimethyl sulfoxide (DMSO, 99.9%) were purchased from Sigma-Aldrich Company Ltd (Dorset, UK). Tween 80 was purchased from Cambridge Bioscience (Cambridge, UK). Commercial sunflower oil (Flora Food Group, Amsterdam, Netherlands) was purchased from a supermarket. Potassium hydroxide (KOH, pellets, ACS reagent, >85% purity), hydrochloric acid (HCl, analytical reagent grade, S.G. 1.18, ~37%), and sodium hydroxide (NaOH, analytical reagent grade, pellets) were purchased from Thermo Fisher Scientific (Loughborough, UK). Pepsin (from porcine gastric mucosa, lyophilized powder, 500 U/mg), pancreatin (from porcine pancreas, 8 USP) and bovine bile (dried, unfractionated) were purchased from Sigma-Aldrich (Dorset, UK). Salts to prepare digestive buffers, i.e., potassium chloride (KCl), potassium dihydrogen sulfate (KH_2PO_4), sodium bicarbonate ($NaHCO_3$), sodium chloride (NaCl), magnesium chloride hexahydrate ($MgCl_2(H_2O)6$), ammonium carbonate ($(NH_4)_2CO_3$), and calcium chloride dihydrate ($CaCl_2(H_2O)2$) were purchased from Sigma-Aldrich. A total starch assay kit (K-TSTA-100A) was purchased from Megazyme Ltd (Bray, Ireland). HPLC grade methanol (>99.9%), acetonitrile (>99.9%), ethyl acetate (>99.7%), curcumin, demethoxycurcumin, and bisdemethoxycurcumin were purchased from Sigma Aldrich. Formic acid (for mass spectrometry) was purchased from Honeywell (Seelze, Germany). All solutions were prepared with pure deionized water (with a resistivity of not less than 18.4 MΩ cm at 25°C) (Merck Millipore, Darmstadt, Germany).

Methods

Encapsulation of curcumin: Preparation of Cur-γ-CD-MOFs: The preparation of γ-cyclodextrin metal-organic frameworks (γ-CD-MOFs) and their encapsulation of curcumin were conducted following established methods and full details are given in previous publications [7-12]. Briefly, the process involved dissolving γ-CD and KOH in deionized water, filtering and allowing methanol diffusion into the sample for 7 days. The crystals were then dried under vacuum at 30°C overnight (Genevac EZ-2 Plus Evaporating System, Marshall Scientific, New Hampshire, USA). Curcumin was encapsulated into the CD-MOFs using an impregnation method, in which a 10:1 molar ratio of γ-CD-MOFs to curcumin was simultaneously dispersed and dissolved in methanol. Subsequently, the mixture was centrifuged, washed with methanol to remove the non-encapsulated fraction of curcumin, and then dried overnight under vacuum, yielding Cur-γ-CD-MOFs.

Preparation of coarse emulsions: Curcumin was dissolved in sunflower oil to a final concentration of 2 mg/mL under magnetic stirring for 30 min. NaCas was dissolved in water 3% w/w and oil-in-water emulsions (80:20 w/w) were prepared by homogenizing the oil and NaCas solution via an Ultra Turrax T25 homogenizer (IKA-Werke GmbH & Co., Staufen, Germany) at 21,000 rpm for 1 min. Emulsions where Cur-γ-CD-MOFs were dispersed in the oil phase were prepared in the same way. In the remainder of this work these are referred to as MOF/Cas emulsions, whereas the former are referred to as Cur/Cas emulsions. Emulsions were also prepared in exactly the same way but using 3% w/w Tween 80 as the emulsifier, referred to below as Cur/T80 and MOF/T80 emulsions.

***In vitro* gastrointestinal digestion (static model)**: A static *in vitro* digestion model was conducted according to the INFOGEST digestion model published by [13].

Oral phase: exactly 5 mL of emulsion was mixed with 4 mL of SSF at pH 7, 25 µL of 0.3 M $CaCl_2$, and 0.975 µL of dH_2O in a 50 mL Falcon tube. The digestion tube was incubated in a shaking incubator (Incu-Shake MAXI, SciQuip Ltd, Shropshire, UK) operated at 37°C, 115 rpm. The salivary amylase was omitted because of the expected short residence time (< 1 min).

Gastric phase: The subsequent 10 mL of oral sample was mixed with 8 mL of SGF at pH 3, 0.5 mL of pepsin (2000 U/mL) and 5 µL of $CaCl_2$ (0.3 M). The pH was adjusted to pH 3 using 1 M HCl solution. The solution was then incubated for 2 h.

Intestinal phase: A similar volume of SIF electrolyte was added to the above gastric 'chyme'. This was followed by the addition of 40 µL of $CaCl_2$ (0.3 M), and 3 mL of bile (10 mM) and 5 mL of pancreatin solution (100 U/mL trypsin activity) that were made up in SIF electrolyte solution. Once the pH was adjusted to 7 with a 1 M NaOH solution, the sample was further incubated for 2 h.

An important but slight variation from the protocol was adapted for samples containing non-encapsulated curcumin and Cur-γ-CD-MOFs. It was assumed that these samples would be delivered in a capsule form that would ensure that they remained intact until reaching the intestinal phase. Therefore, enzymes relating to the oral phase (salivary amylase) and gastric phase (pepsin) were omitted in the 'digestion' of these vehicles. The volumes of curcumin of each of the samples were adjusted to ensure that all had the same starting concentration of a curcumin, $C_{initial}$ = 2 mg/mL.

Droplet size measurements: Static light scattering (SLS) was used to measure the particle size distribution (PSD) of the emulsions via a Malvern Mastersizer 3000 (Malvern Instruments, Worcestershire, UK) assuming a refractive index and absorption of the dispersed phase of 1.47 and 0.01, respectively. The mean particle size of the emulsions was reported as volume mean diameter (d_{43}) since this is more sensitive to droplet aggregation.

ζ-potential measurements: The ζ-potentials of aqueous dispersions of the non-emulsion and emulsion samples were determined via a Zetasizer (Nano ZS series, Malvern Instruments, Worcestershire, UK) at 25 °C with the use of a folded capillary cell (Model DTS 1070, Malvern Instruments, Worcestershire, UK). Samples before and after *in vitro* digestion were collected at appropriate time intervals and were either dispersed in phosphate buffer (pH 7.0) or SGF buffer (pH 3.0) or SIF buffer (pH 7.0).

***In vitro* release and bioaccessibility of CUR**: The amount of curcumin released from the curcumin-loaded delivery systems in comparison to native (non-encapsulated) curcumin was measured during *in vitro* gastrointestinal digestion. The sampling was set at every 1 h of gastric conditions and/or at 20 min intervals during intestinal conditions. The bioaccessibility of curcumin was determined for all digesta at the end of the 2 h of intestinal phase. Each sample was centrifuged at 20,000 × g for 10 min at 4°C. Any curcumin that was 'solubilized' and therefore potentially bioaccessible was assumed to be present within the middle layer of supernatant fraction, i.e., not present as a sediment of large particles at the bottom of the tube, nor trapped in any oil layer at the top. We assume that such material is held in some sort of complex mixed bile salt micelles and for brevity we therefore refer to the concentration of curcumin in this layer as $C_{micelle}$. Curcumin in this middle layer was therefore extracted with 500 µL ethyl acetate, three times. The ethyl acetate was evaporated off under vacuum and the precipitated curcumin was re-dissolved in acetonitrile. The concentration of curcumin in these acetonitrile solutions was analyzed using ultra high-performance liquid chromatography (UHPLC) analysis, using an Agilent 1260 Infinity II LC system coupled with DAD detector. The measurement wavelength was 425 nm and the separation column was an Ascentis Express C18 (150 mm × 4.6 mm, 2.7 µm) fitted with a Phenomenex guard column. The mobile phase A was 0.1% aqueous formic acid, the mobile phase B was 0.1% formic acid in acetonitrile. A flow rate of 1 mL/min and a maximum pressure limit of 400 bar was used for elution. The gradient elution program was: 0 min, 82% of A; 10.8-16.8 min, 68% of A; 16.8-19.2 min, 40% of A; 19.2-21.7 min, 0% of A; 21.7-23.8 min, 82% of A. The injection volume was 10 µL and the column temperature was maintained at 35°C. External curcuminoid standards bisdemethoxycurcumin, demethoxycurcumin and curcumin were used to quantify the elution peaks via a calibration curve in acetonitrile ranging in curcuminoid concentrations from 0.1 µM to 20.0 µM. The resultant % Bioaccessibility of curcuminoids was thus calculated as:

$$\text{Bioaccessibility} = [c_{micelle} / c_{initial}] \times \text{dilution factor} \times 100 \quad (1)$$

Glucose release: The glucose released during the *in vitro* gastrointestinal digestion was quantified by using a total starch assay kit (AOAC Method 76-13.01), with slight modification, to assess the breakdown of γ-CD-MOFs. Digesta samples were collected at 1 h intervals in the gastric phase and at 20 min intervals in the intestinal phase. After centrifuging the digesta at 10,000 rpm for 15 min, 50 µL of supernatant, in duplicate, was pipetted into a test tube and mixed well with 5 mL of sodium acetate buffer. After storage at 50°C in a water bath for 10 min, 50 µL of amyloglucosidase was added to one sample tube and 50 µL of buffer was added to the other (control tube). The tubes were then incubated for a further 30 min at 50°C. Once cooled, 1 mL of each solution was centrifuge at 13,000 rpm for 5 min. This was followed by the transfer of 50 µL of supernatant to 2 fresh test tubes and the addition of 1.5 mL GOPOD (Glucose Oxidase/Peroxidase) reagent. After

further incubation at 50 °C for 20 min, the absorbance at 510 nm was measured and compared against that for a series of standard glucose solutions against the reagent blank using Tecan Spark 10M plate reader (Zürich, Switzerland).

***Ex vivo* intestinal transport and absorption of curcumin using mouse jejunum**: The *ex vivo* intestinal transport study protocol used was previously reported by Niaz and Mackie [14], which utilized an Ussing chamber and mouse jejunum. Intestinal tissue was obtained from 6-week-old C57BL6 mice that had been freshly anesthetized, provided by the Central Biomedical Services, University of Leeds, UK. The protocol was approved by the University of Leeds Animal Welfare Ethical Review Board and was conducted under the appropriate license (PEL number: XDE639D76) in accordance with the UK Home Office Animals Scientific Procedures Act (ASPA) 1986.

Following extraction, the intestinal tissue was rinsed twice with ice-cold Krebs-Ringer bicarbonate (KRB) solution and immediately immersed in cold D-glucose solution (10mM, pH 7.4) before being placed on ice for no longer than 30 min prior to use. A 2 cm of intestinal segment was excised from the jejunum, and the serosal layer was removed. The tissue was then secured onto a cassette and positioned between two chambers, ensuring the mucosal side faced the apical chamber while the serosal side was oriented towards the basolateral chamber. To each chamber, 1 mL of the respective solution was added: Ringer's solution with glucose for the apical chamber and Ringer's solution with mannitol for the basolateral chamber. Transepithelial electrical resistance (TEER) values were continuously monitored throughout the experiment, with any intestinal tissue displaying a TEER measurement below 20Ωcm^{-2} considered not viable and excluded from further analysis.

The absorption study was carried out on the native curcumin dispersions, Cur- γ-CD-MOFs samples and the Cur/Cas and MOF/Cas and emulsions. Prior to injection into the apical side of the Ussing chamber, samples were subjected to gastrointestinal digestion (as described in section 2.2.5) and 0.5 mL of digesta collected at the endpoint of digestion were added to the chamber. At 60 and 120 min, 500 µL of sample was collected from each chamber and replaced with equal volumes of corresponding buffer. The jejunum tissue was also collected at the end of the experiment. Curcuminoids were extracted from the samples and quantified as described above.

Optical microscopy: The microstructure of samples was imaged using a light microscope (Nikon, SMZ-2T, Tokyo, Japan) equipped with a digital camera (Leica MC120 HD).

Confocal scanning laser microscopy (CLSM): Confocal laser scanning microscopy (CLSM) was carried out using a Zeiss LSM880 upright Airyscan microscope (Cambridge, UK) with a 10 x/0.30 and 20 x/0.8 objective lens. After washing the jejunum tissue with PBS (phosphate-buffered saline) from the absorption studies with Cur-γ-CD-MOFs samples, the tissue was fixed on a microscope slide using 4% PFA solution for 3 h. Nile Red (1 g/mL in DMSO) was used to stain the tissue, using an excitation wavelength of 561 nm and emission wavelength of 665 nm. For curcumin identification its natural fluorescence was used, via excitation and emission wavelengths of 488 nm and 544 nm, respectively. Images were processed using the image analysis software Fiji [15].

Statistical analysis: Statistical analysis was carried out using OriginPro 2024b (OriginLab, Northampton, USA) and statistical significance was taken at $p < 0.05$. Data were collected in triplicate. Results in tables are expressed as means ± standard deviations, the latter represented in figures by the error bars.

RESULTS AND DISCUSSION

Particle sizes of emulsions stabilized by sodium caseinate and Tween 80

The volume mean diameter (d_{43}) and droplet size distributions of the four coarse emulsions, supplemented by corresponding microscopy images, are summarized in Table 1 and depicted in Figure 1. The initial droplet size range (approx. 25 µm) was within the typical range of macroemulsions (0.5 – 100 µm) [16]. When the pH was reduced to 3 in the gastric phase, the droplet size of emulsions stabilized by NaCas increased significantly and remained high throughout the 2 h duration of gastric conditions. Upon transitioning to the intestinal phase (pH 7), the droplet size of the NaCas-stabilized emulsions decreased significantly, reducing to approximately half of their size observed in the gastric phase. In contrast, emulsions formulated with Tween 80 exhibited no significant change in droplet size during the gastric phase, but their size gradually increased during the intestinal phase. The significant increase in d_{43} with NaCas during simulated gastric conditions can be largely attributed to the destabilization of the emulsion system due to the presence of pepsin. Pepsin cleaves the interfacial NaCas, breaking down the protein layer, contributing to droplet coalescence [17,18]. The proteolysis of the interfacial film has weakened capabilities of steric stabilization and electrostatic repulsion because any remaining adsorbed

Table 1: Mean droplet size of initial emulsions and as emulsions undergo *in vitro* gastrointestinal digestion.

Samples	d_{43} (μm)				
	Initial	Gastric phase		Intestinal phase	
	0 min	60 min	120 min	180 min	240 min
Cur/Cas	26.1 ± 1.6[a]	221.0 ± 100.3[a]	131.3 ± 44.5[a]	37.9 ± 2.9[a]	125.2 ± 96.0[a]
MOF/Cas	26.0 ± 1.3[a]	217.7 ± 46.4[a]	228.2 ± 34.7[a]	79.0 ± 47.8[b]	55.8 ± 6.4[b]
Cur/T80	23.8 ± 0.1[b]	21.6 ± 0.2[b]	24.5 ± 1.6[b]	39.8 ± 23.0[a]	46.4 ± 8.0[c]
MOF/T80	23.7 ± 1.8[b]	20.9 ± 1.6[b]	25.9 ± 1.1[c]	33.6 ± 2.69[a]	42.5 ± 5.8[c]

Values expressed as mean ± standard deviation. [a-c] Different lower-case letters indicate a statistically significant difference down the column in different GI phases ($p < 0.05$).

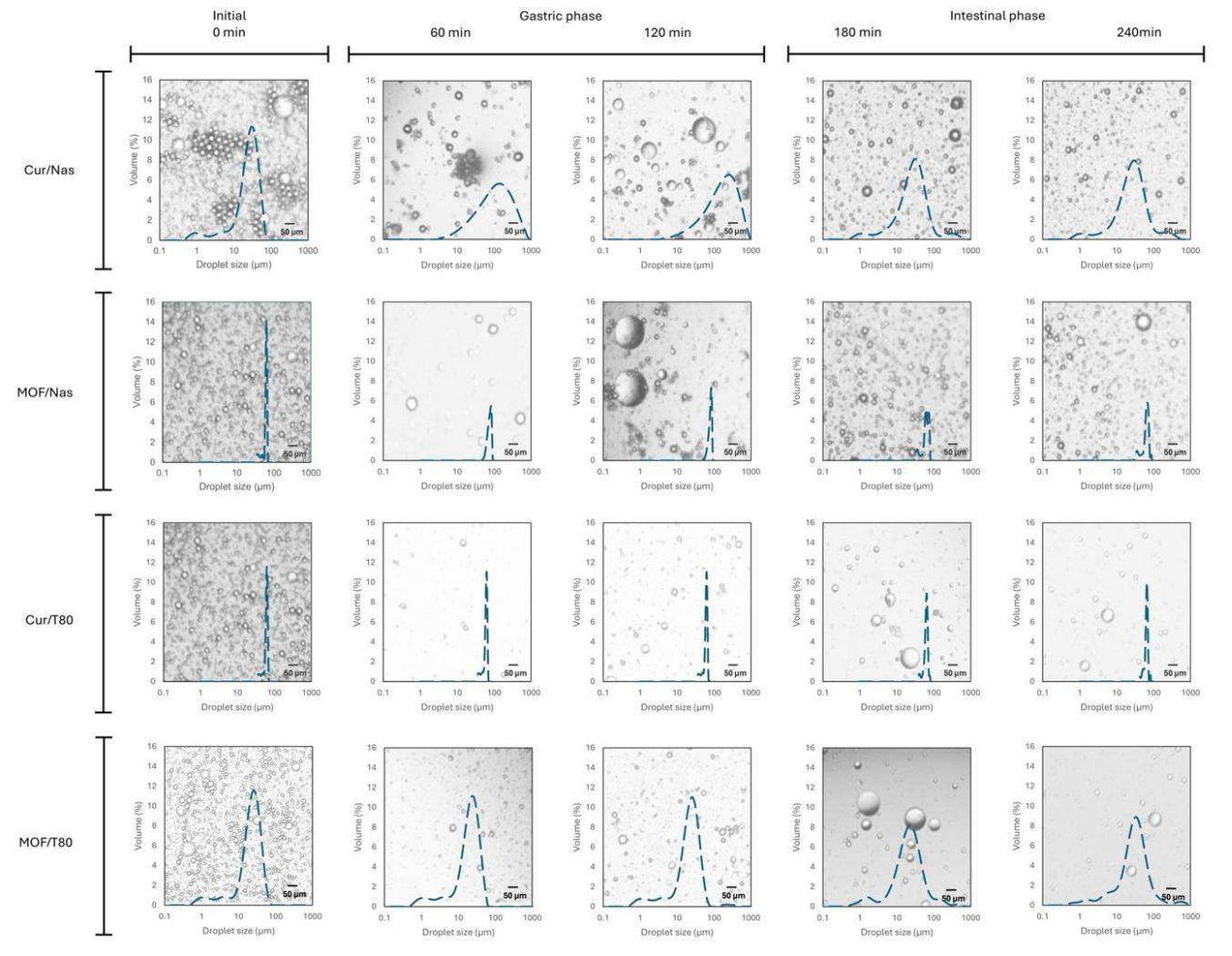

Figure 1 Microscopy images with superimposed droplet size distributions of the initial emulsions and after their exposure to 60 and 120 min of gastric phase, followed by intestinal conditions, at 180 and 240 min, of simulated digestion.

protein fragments will be shorter and/or may no longer carry enough charge. Precipitation of the NaCas can occur as the pH approaches its isoelectric point (pI, ~ 4.6) [16-20]. Even though the NaCas starts to become (positively) charged again at pH 3, the net charge on the adsorbed protein is still lower than at pH 7, leading to diminished electrostatic repulsion between droplets, promoting droplet flocculation and coalescence [21].The relatively high ionic strength – primarily contributed by the level (47.2 mM) of NaCl but also due to the presence of other salts in the gastric phase – exacerbates emulsion destabilization via electrostatic screening effects [22,23]. Additionally, the presence of the divalent cations, $Mg2^{+}$ and $Ca2^{+}$ can further destabilize the emulsions via ionic bridging [24,25].

The reduction of droplet size of NaCas-stabilized emulsions in the intestinal conditions can be attributed to the restoration of NaCas solubility at neutral pH, as well as re-established surface charge and hence higher electrostatic repulsion [16-26], even though the ionic strength remains high. However, the addition of pancreatin, containing a mixture of lipolytic and proteolytic enzymes in the intestinal phase also influences the droplet size. The lipases hydrolyze triglycerides in the oil droplets to monoglycerides and free fatty acids (FFAs) that act as natural low molecular weight emulsifiers, helping to stabilize smaller droplet sizes [18-28]. As digestion progresses, proteolytic breakdown of NaCas may also further reduce its emulsion stabilizing capacity as adsorbed chains become even shorter and/or less charged [29,30]. It has also been suggested that other lipid digestion products, such as micelles and vesicles formed from bile salts, FFAs, and monoglycerides, may aggregate with the remaining oil droplets and give the appearance of larger overall 'droplet' (particle) sizes [31,32].

The Tween 80-stabilized emulsions were much more stable to the raised acidity and ionic strength of gastric conditions due the non-ionic nature of Tween 80 [33]. Tween 80 provides purely steric repulsion, its hydrophilic 'head' extending into the aqueous phase and its hydrophobic tail anchored in the oil phase [34], whilst it is also not susceptible to enzymatic breakdown. Nevertheless, a slight increase in droplet size was observed as the intestinal phase progressed. This may have been due to droplet aggregation with lipolysis products, as mentioned above, and/or displacement of Tween 80 from the interface by these products, causing partial coalescence and larger droplet size [35].

ζ-potentials of emulsions stabilized by sodium caseinate and Tween 80

The ζ-potential measurements corroborated the emulsion stability changes indicated by the particle size measurements described above. A higher absolute ζ-potential value is generally an indication of stronger charge (negative or positive) on the particle surface and therefore a greater degree of electrostatic repulsion between the particles, thereby reducing the likelihood of aggregation [36]. As expected, emulsions formulated with NaCas exhibited a shift in ζ-potential from negative (-20 to -30 mV) to positive (15 – 20 mV) under gastric conditions, followed by a return to a lower magnitude negative value (~ -10 mV) during the intestinal phase (Figure 2), considering the pI of the adsorbed protein. Although Tween 80 is a non-ionic surfactant, emulsions formulated with Tween 80 showed a moderately negative ζ-potential (~ -25 mV) during the gastric phase, that decreased to ~ -10 mV in the intestinal phase.

The initial negative charge with Tween 80 might be due co-adsorption of surfactant impurities or the preferential adsorption of hydroxyl ions from water [37,38]. Or other anions, whilst the moderate changes during digestion were probably due to adsorption of components released during the digestion. The slight lowering of the ζ-potential during the intestinal phase probably contributed to the increased droplet aggregation and/or coalescence observed. Thus, the changes in ζ-potential and therefore electrostatic repulsion coincided with observed droplet coalescence and as described in the particle sizing section above.

Controlled release and bioaccessibility

The bioaccessibility of curcuminoids from emulsion systems was assessed in comparison to native curcumin and Cur-γ-CD-MOFs and the results are summarized in Figure 3. According to Górnicka et al. [4], the solubility of curcumin in water is poor - approximately 0.6 μg/mL. With the presence of bile salts within the simulated intestinal fluid, the apparent solubility of curcuminoids increased to nearly 60 μg/mL, increasing the bioaccessibility to 3.6%. In the NaCas-stabilized emulsions, the bioaccessibility of curcuminoids tripled, to 11.9% compared to this 3.6 % 'baseline' level, and increased 5x to 19.2 % in the Tween 80-stabilized emulsions. Amongst all the samples, the curcuminoids "released" from the Cur-γ-CD-MOFs demonstrated the highest bioaccessibility, at 21.3%. However, incorporating the Cur-γ-CD-MOFs into the emulsions (MOF/Cas and MOF/T80) adversely affected curcumin delivery, with less than 5% of curcuminoids remaining bioaccessible – Figure 3. Based on Figure 4A, it can be said that sustained release – characterized by a gradual and prolonged release of curcuminoids over time – was observed for Cur-γ-CD-MOFs alone and both curcumin emulsion samples (Cur/Cas and Cur/T80). However, this release profile was not observed in emulsions containing Cur-γ-CD-MOFs (MOF/Cas and MOF/T80). Moreover, the % release of curcuminoids for MOF/Cas was slightly lower and for MOF/T80 only slightly higher than native non-encapsulated curcumin.

To further investigate the mechanism of release of curcuminoids from systems containing Cur-γ-CD-MOFs, glucose levels in the digesta were quantified, since the amylases present will digest the γ-CD to linear or branched oligosaccharides and so degrade the γ-CD-MOFs [39-41]. The results (Figure 4B), indicated that nearly all γ-CD-MOF was degraded in emulsion samples, whereas only approximately half the γ-CD-MOF appeared to be degraded

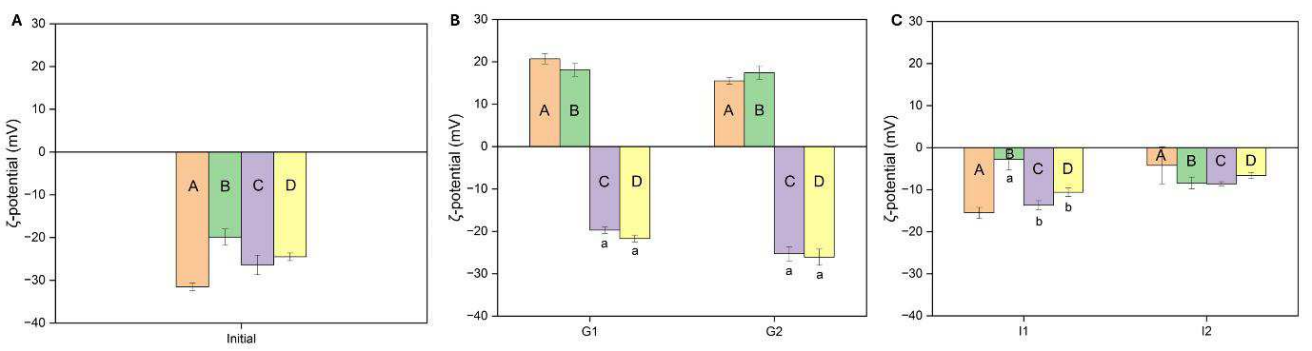

Figure 2 Measured -potential of emulsions (A) pre-digestion (initial) and at hourly intervals during simulated gastrointestinal digestion during (B) gastric phase and (C) intestinal phase. Columns A (orange) represents sodium caseinate-stabilized emulsion incorporating curcumin, B (green) represents sodium caseinate-stabilized emulsion incorporating Cur-γ-CD-MOFs, C (purple) represents Tween 80-stabilized emulsion incorporating curcumin, and D (yellow) represents Tween 80-stabilized emulsion incorporating Cur-γ-CD-MOFs. Columns with different letters represent significant difference within each group of 4 samples at $p < 0.05$.

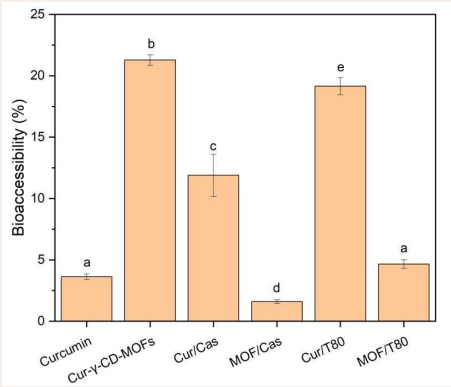

Figure 3 Bioaccessibility of total curcuminoids after in vitro gastrointestinal digestion of: curcumin, Cur-γ-CD-MOFs and sodium caseinate-stabilized emulsions incorporating curcumin and Cur-γ-CD-MOFs; Tween 80-stabilized emulsions incorporating curcumin and Cur-γ-CD-MOFs. Columns with different letters represent significant difference within each group of 4 samples at $p < 0.05$.

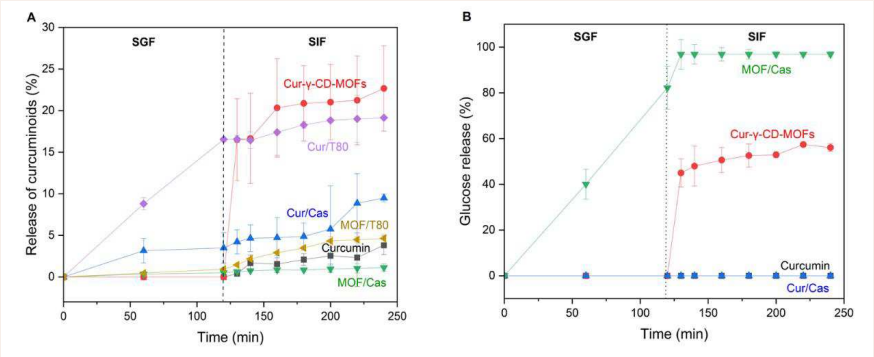

Figure 4 (A) *In vitro* controlled release of curcuminoids from native curcumin, Cur-γ-CD-MOFs and emulsion systems and (B) Glucose released during *in vitro* gastrointestinal digestion. The symbols ● represents Cur-γ-CD-MOFs, ◆ represents Tween 80-stabilized emulsion incorporating curcumin, ▲ represents sodium caseinate-stabilized emulsion incorporating curcumin, ◀ represents Tween 80-stabilized emulsion incorporating Cur-γ-CD-MOFs, ▪ represents curcumin and ▼ represents sodium caseinate-stabilized emulsion incorporating Cur-γ-CD-MOFs.

in the non-emulsion samples. The reasons for this are not clear, but it is possible that γ-CD-MOFs interact with the surface of the emulsion droplets, and this somehow facilitates access of the enzymes degrading the system.

Tween 80 is more effective in reducing the interfacial tension than NaCas [42,43]. Due to its lower molecular weight and ability to pack more tightly together at interfaces. This facilitates smaller droplet sizes and therefore better dispersion of curcuminoids dissolved in the oil, enhancing their bioaccessibility because smaller droplets mean a higher interfacial area and thus more efficient lipolysis [44]. In addition, the non-ionic nature of Tween 80 makes it relatively stable to changes in pH and salt concentration, unlike protein-based emulsifiers such as sodium caseinate. This stability across gastrointestinal conditions helps emulsion integrity and allows more consistent micellization and therefore solubilization of curcumin, ultimately enhancing bioaccessibility.

Post-synthesis, the permanent porosity of γ-CD-MOFs enables encapsulation of bioactive compounds like curcumin, which can contribute to their improved solubility and bioaccessibility [41-46]. Most studies suggest that curcumin is encapsulated within the hydrophobic cavity of the γ-CD or held between γ-CD pairs via hydrogen bonding [7-48]. In many cases, the relatively weak metal-ligand coordination bonds are susceptible to rapid degradation in aqueous environments. According to Feng et al. [49], water molecules displace the metal-linker coordination bonds of MOFs, initiating hydrolysis that disrupts the structure. The stability of MOFs is dependent on the charge density of the metal ions, strength of coordinating bonds, and ligand configuration [50]. Low-valency metal ions tend to form MOFs with weaker coordinate bonds since it generally requires fewer linkers to balance the charge. Conversely, to balance the charges with higher valency metal ions more linkers are required, which can lead to higher coordination number of metal clusters and enhance the MOF stability. Moreover, it has been reported that MOFs with larger cavities and longer linkers are less stable due to a more open structure and lower density. This exposes the MOF to easier attack from the water molecules [49]. For this reason, α-CD and β-CD are more water-resistant than γ-CDs due to their smaller inner cavities [51,52]. Degraded γ-CD-MOFs are thought to rapidly release the trapped curcumin from within the γ-CD cavities which then, the absence of any other components, transforms to its insoluble crystalline form or be solubilized to some extent within the mixed 'micelles' formed by the bile salts and any associated lipids or lipid degradation products formed during digestion [8]. The micelle-solubilized curcumin is presumed to be far more bioaccessible. It is likely that the curcumin held tightly between hydrophilic γ-CD pairs also contributed to the improved apparent solubility of curcumin, leading to its improved bioaccessibility. Thus, these two release locations may together be responsible for the sustained release observed in the case of Cur-γ-CD-MOFs alone. Because γ-CD is also susceptible to amylolytic hydrolysis, there should be a further slight increase in apparently solubilized curcuminoids during intestinal digestion, as observed here and in agreement with the observations of Lv et al. [53]. This further indicated that the pores of the γ-CD-MOFs could be slowly hydrolyzed, releasing curcumin gradually over time. It is interesting, however, that even at the end of the intestinal digestion, at least 40% of the expected glucose content of the Cur-γ-CD-MOFs had still not been released. Thus, the Cur-γ-CD-MOFs are more resistant to degradation than expected for γ-CD-MOFs and a gradient of concentration from the γ-CD-MOFs to mixed micelles may still be governing the rate of release of curcuminoids. Interestingly, confocal microscopy revealed that in the emulsion systems the Cur-γ-CD-MOFs were mainly situated at the oil-water interface (**Figure S1**). This was surprising since the exterior of γ-CD-MOFs is expected to be hydrophilic and so they should preferentially stay within the aqueous phase. This adsorption to the interface somehow seems to facilitate either the dissolution of the Cur-γ-CD-MOFs and/or the release of curcumin molecules from them, that results in less bioaccessible (i.e., less micelle-solubilized) curcumin and therefore presumably more large crystals that sediment out.

Cur-γ-CD-MOFs are likely to be quite unstable to gastric conditions (pH 3), depending on the composition and coordination of the metal centers. At low pH, H^+ ions could potentially compete with K^+ ions for binding sites on the cyclodextrin (ligand) in the MOF structure, leading to the structural instability and degradation of the MOF [54]. This is largely due to the coordination between monovalent K^+ and cyclodextrin being relatively weak compared to that of higher valency metal species, which could form stronger metal–ligand bonds that may be more resistant to proton displacement in acidic environments. In addition, hydroxyl groups within cyclodextrin can be protonated at low pH [49,50]. This can further alter the γ-CD structure and be detrimental to the stability of MOF. Thus, γ-CD was quantifiable as glucose even in the absence of amylase due to the disassociation of MOFs. Any re-stabilized oil droplets formed at the end of the intestinal phase probably cannot efficiently solubilize any curcumin released from the Cur-γ-CD-MOFs, whilst they curcuminoids themselves may also begin to degrade at the more alkaline pH of the intestinal digesta. Overall then, incorporating Cur-γ-CD-

MOFs into oil-in-water emulsions does not seem to be particularly advantageous in terms of improving delivery of active curcuminoids. However, the proposed initial delivery is a capsule form that would protect the Cur-γ-CD-MOFs during the gastric phase.

Since the Tween 80-stabilized emulsions containing Cur-γ-CD-MOFs did not perform any better than NaCas-stabilized emulsions, the degradation of the Cur-γ-CD-MOFs within them was assumed to be similar and thus there does not seem to be any particular advantage of using a synthetic, non-digestible low molecular weight emulsifier.

Ex vivo transport via intestinal mucosa

Post-digestion, the bioaccessibility data discussed above suggest that the increasing levels of curcuminoids released and available for intestinal absorption should be in the following order: MOF/Cas < Curcumin < Cur/Cas < Cur-γ-CD-MOFs. To be bioaccessible, compounds must be transported from the apical side of intestinal epithelia cells to the basolateral side to enter systemic circulation [3]. Therefore, absorption experiments were performed to assess the transport and absorption of curcuminoids via intestinal epithelial cells (from mice, as described in the Materials and Methods). The results obtained (Figure 5), of the concentration of curcuminoids on the apical and basolateral sides of the tissue and within the tissue itself, indicate an almost identical sequence in terms of increasing uptake: Curcumin < MOF/Cas < Cur/Cas < Cur-γ-CD-MOFs.

According to the literature, curcuminoids are best absorbed in the upper part of small intestine, and least favored in ileum, with no significant difference in the intestinal regions between the duodenum and jejunum [55]. For this reason, the jejunum section of the mouse intestine was selected for use in the Ussing chamber. Pure curcumin is naturally poorly soluble in water and exhibits low permeability across intestinal barriers. The exact absorption mechanism of solubilized curcumin remains unclear. Caco-2 cell monolayers have been widely used to determine the permeation rate and mechanism of curcumin uptake. Studies suggest that curcumin absorption occurs via both passive (diffusive) and carrier-mediated active transport (2,3,55,56,67). Curcumin is thought to be a substrate of P-glycoprotein (P-gp) and so curcumin transport may be affected by P-gp efflux, which pumps drugs out of cells, thus reducing absorption [55,56]. Curcumin has also been proposed to function as an inhibitor of the efflux transporter P-gp and Multidrug Resistance Protein (MRP), potentially improving the absorption and bioavailability [39,57,58]. However, these studies were conducted using various types and concentration of co-administered substrates and source of cells, making it challenging to compare.

Bioaccessibility has been reported as being slightly improved by incorporation into bile salt mixed micelles but absorption is predicted to remain poor, consistent with the observed results [59]. It has been suggested that an oil droplet dominant formulation may be more advantageous [60]. When incorporated into an oil-in-water emulsion, higher absorption might be related to lipolysis and the formation of a higher concentration and richer range of

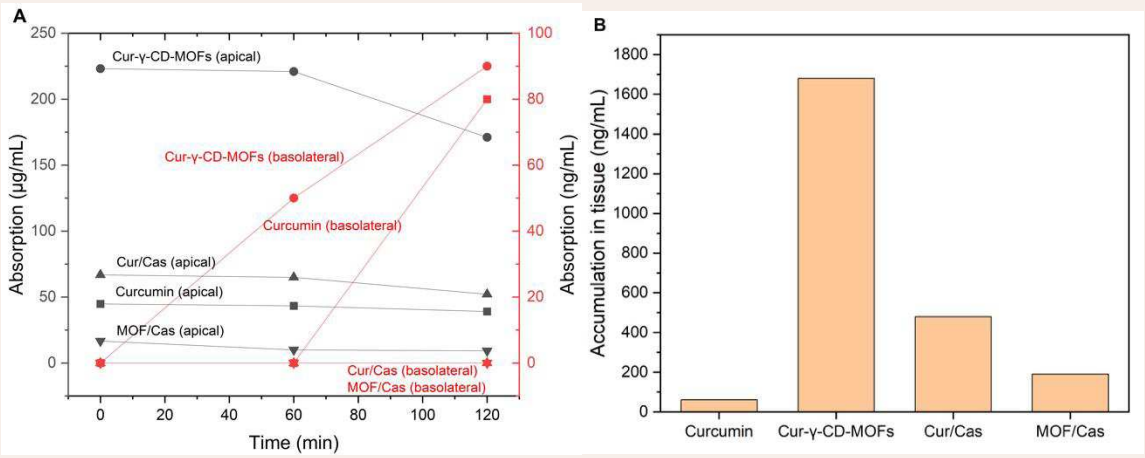

Figure 5 (A) Absorption of curcuminoids across mouse jejunum in an Ussing chamber for 4 different delivery systems with black lines representing the apical side and red lines representing the basolateral side. The symbols ● represents Cur-γ-CD-MOFs, ▲ represents sodium caseinate-stabilized emulsion incorporating curcumin, ■ represents curcumin and ▼ represents sodium caseinate-stabilized emulsion incorporating Cur-γ-CD-MOFs. (B) The concentration of curcuminoids accumulated within the jejunum tissue.

composition of mixed micelles, better able to accommodate curcuminoid molecules.

The bioavailability of bioactive compounds forming inclusion complexes with γ-CD-MOFs has been described as enhanced due to their improved apparent solubility [61,62]. Encapsulation within CD-MOFs was described as a multi-phase system in which free curcumin, free cyclodextrins, drug entrapped in CD complexes, and dispersed drug within solution exists in equilibrium [63]. Topuz and Uyar [52] noted that hydrophilic γ-CDs may not easily traverse the gastrointestinal mucosa, and their presence does not directly influence the permeability of incorporated compound through the mucosa. This was in agreement of a study conducted by Nasr et al. [64], where unlike α- and β-CD, γ-CD induces only a weak membrane permeability, because its larger cavity does not effectively extract phospholipids from membranes. Conversely, the curcumin-CD complexes act as a delivery reservoir, maintaining a constant free curcumin concentration for diffusion across the intestinal membrane. Although the MOF/Cas emulsion yielded lower bioaccessibility than pure curcumin (Figure 3), the solubilization effect of γ-CD-MOFs likely contributed to higher absorption (Figure 5B). Prolonged release of curcuminoids at the absorption site may enhance absorption via a combined effect of bioaccumulation by passive diffusion and active transport across the membrane in a concentration-dependent manner. It should also be noted that the starting concentration on the apical side for all samples is directly related to the bioaccessible fraction of curcuminoids as the endpoint of *in vitro* gastrointestinal digestion and differs due to the variation in delivery systems. These differences do not directly influence the absorption of curcuminoids across the intestinal tissue. By the end of the experiment, in the majority of observations, the curcuminoids were found in the tissue (Figure 6). These results suggested that curcuminoids directly released from γ-CD-MOFs or transported via the intermediary of mixed micelles could accumulate in the intestinal epithelial layer. This accumulation may retard further absorption from the gut and increase the residence time of curcuminoids within the mucus, thereby prolonging their bioactive effects [14]. The accumulation was more prominent in Cur-γ-CD-MOFs as the average particle size of the bioaccessible fraction within the supernatant layer was below 200 nm (**Table S1**), and within the reported range of pore size of gastrointestinal mucus of 100 – 200 nm [65]. However, this

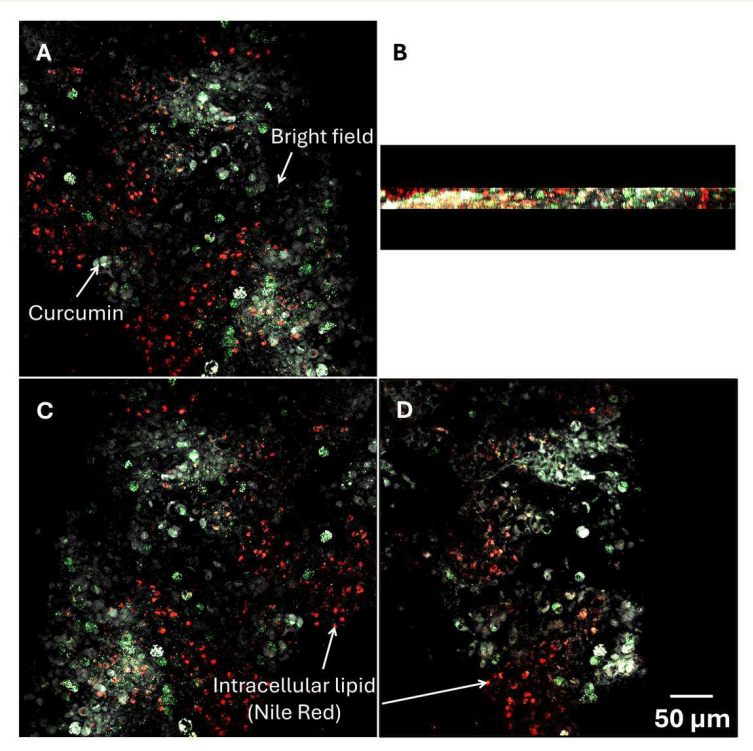

Figure 6 Confocal micrographs illustrating the absorption of curcuminoids from cur-γ-CD-MOFs across mouse jejunum from (A) apical side to (C) basolateral side. (B) = cross-section on z-plane and (D) two-dimensional microscopy image of the absorption in the tissue. The red represents the intracellular lipid stained by Nile Red, the green represents the natural fluorescent curcumin, and grey scale represents the bright field.

may not be the case for some coarse emulsions since the droplet size appeared to exceed this range. A reduction in particle sizes to < 200 nm may therefore promote diffusion across intestinal epithelial cells via transcellular uptake.

CONCLUSIONS

The application of highly porous γ-CD-MOFs in biological and medical applications (i.e., drug release) requires excellent chemical stability, including strong resistance to hydrolysis or structural collapse in physiological environments. Although the stability of γ-CD-MOFs may be less than desirable, the method of delivery plays a critical role in determining their rate of degradation and therefore enhancement of both the bioaccessibility and transepithelial absorption of curcumin encapsulated within them. If delivered in capsule form, Cur-γ-CD-MOFs would be protected from the acidic gastric environment that could otherwise degrade γ-CD-MOFs and destabilize any emulsions into which they have been incorporated. This would allow γ-CD-MOFs to increase the apparent solubility of curcumin in a sustained manner, thus resulting in a higher absorption rate. Prolonged solubilization of curcumin could potentially persist into the colon, where fermentation occurs. Consequently, the fate of γ-CD-MOFs and unabsorbed curcumin in an ex vivo fermentation model presents an opportunity for future research.

AUTHOR CONTRIBUTIONS

J.X.O. – conceptualization, methodology, software, validation,formal analysis, investigation, resources, data curation, writing – original draft preparation, review and editing, visualization; A.R.M. – conceptualization, methodology, validation, resources, writing – review and editing, supervision, funding acquisition; R.E. – conceptualization, methodology, validation, resources, writing – review and editing, supervision, funding acquisition; T.N. – methodology, writing – review and editing, supervision; B.S.M. – conceptualization, methodology, validation, resources, writing – review and editing, supervision, project administration, funding acquisition. All authors have read and agreed to the published version of the manuscript.

ACKNOWLEDGEMENTS

The authors gratefully acknowledge the assistance provided by Dr. Ruth Hughes in the bioimaging of samples. This work was partly funded via the BBSRC & Innovate UK (grant no. 131860) National Alternative Proteins Innovation & Knowledge Centre (NAPIC).

REFERENCES

1. Nidhi Agrawal, Meenakshi Jaiswal. Bioavailability enhancement of curcumin via esterification processes: A review. Eur J Med Chem Rep. 2022; 6: 100081.
2. Li C, Miao X, Li F, Adhikari BK, Liu Y, Sun J, et al. Curcuminoids: Implication for inflammation and oxidative stress in cardiovascular diseases. Phytother Res. 2019; 33: 1302-1317.
3. Zeng Z, Shen ZL, Zhai S, Xu JL, Liang H, Shen Q, et al. Transport of curcumin derivatives in Caco-2 cell monolayers. Eur J Pharm Biopharm. 2017; 117: 123-131.
4. Górnicka J, Mika M, Wróblewska O, Siudem P, Paradowska K. Methods to Improve the Solubility of Curcumin from Turmeric. Life (Basel). 2023; 13: 207.
5. Zhao J, Jia W, Zhang R, Wang X, Zhang L. Improving curcumin bioavailability: Targeted delivery of curcumin and loading systems in intestinal inflammation. Food Res Int. 2024; 196: 115079.
6. Han Y, Liu W, Huang J, Qiu S, Zhong H, Liu D, et al. Cyclodextrin-Based Metal-Organic Frameworks (CD-MOFs) in Pharmaceutics and Biomedicine. Pharmaceutics. 2018; 10: 271.
7. Oh JX, Murray BS, Mackie AR, Ettelaie R, Sadeghpour A, Frison R. γ-Cyclodextrin Metal-Organic Frameworks: Do Solvents Make a Difference? Molecules. 2023; 28: 6876.
8. Jia X. Oh, Alan R. Mackie, Rammile Ettelaie, Taskeen Niaz, Brent S. Murray. Enhancement of curcumin bioaccessibility: An assessment of possible synergistic effect of γ-cyclodextrin metal–organic frameworks with micelles. Food Res Int. 2025; 205: 115869.
9. Dickinson E. Caseins in emulsions: Interfacial properties and interactions. Int Dairy J. 1999; 9: 305-312.
10. Yan Du, Li-Jun Yin, Qing-Hua Han, Dan Zhao, Hai-Jie Liu. Effect of NaCas/Tween 80 ratios and environmental stresses on the physical stability of perilla oil-in-water emulsions. J Food Processing and Preservation. 2018; 42: e13568.
11. Kaur G, Mehta SK. Developments of Polysorbate (Tween) based microemulsions: Preclinical drug delivery, toxicity and antimicrobial applications. Int J Pharm. 2017; 529: 134-160.
12. Smaldone RA, Forgan RS, Furukawa H, Gassensmith JJ, Slawin AM, Yaghi OM, et al. Metal-organic frameworks from edible natural products. Angew Chem Int Ed Engl. 2010; 49: 8630-8634.
13. Brodkorb A, Egger L, Alminger M, Alvito P, Assunção R, Ballance S, et al. INFOGEST static in vitro simulation of gastrointestinal food digestion. Nat Protoc. 2019; 14: 991-1014.
14. Taskeen Niaz, Alan Mackie. Effect of beta glucan coating on controlled release, bioaccessibility, and absorption of β-carotene from loaded liposomes. Food Function. 2024; 15: 1627-1642.
15. Schindelin J, Arganda-Carreras I, Frise E, Kaynig V, Longair M, Pietzsch T, et al. Fiji: an open-source platform for biological-image analysis. Nat Methods. 2012; 9: 676-682.
16. Xingfa Ma, Dereck E.W. Chatterton. Strategies to improve the physical stability of sodium caseinate stabilized emulsions: A literature review. Food Hydrocolloids. 2021; 119: 106853.
17. Hernan Brice Kenmogne-Domguia, Anne Meynier, Michèle Viau, Geneviève Llamasa, Claude Genot. Gastric conditions control both the evolution of the organization of protein-stabilized emulsions and the kinetic of lipolysis during in vitro digestion. Food Function. 2012; 3: 1302-1309.
18. Malaki Nik A, Wright AJ, Corredig M. Impact of interfacial composition on emulsion digestion and rate of lipid hydrolysis using different in vitro digestion models. Colloids Surf B Biointerfaces. 2011; 83: 321-330.

19. Ha HK, Woo DB, Lee MR, Lee WJ. Development of Hydrophobically Modified Casein Derivative-Based Delivery System for Docosahexaenoic Acids by an Acid-Induced Gelation. Food Sci Anim Resour. 2023; 43: 220-231.

20. Sato ACK, Perrechil FA, Costa AAS, Santana RC, Cunha RL. Cross-linking proteins by laccase: Effects on the droplet size and rheology of emulsions stabilized by sodium caseinate. Food Res Int. 2015; 75: 244-251.

21. Magesh Srinivasan, Harjinder Singh, Peter A. Munro. Sodium Caseinate-Stabilized Emulsions: Factors Affecting Coverage and Composition of Surface Proteins. J Agricultural Food Chem. 1996; 44: 3807-3811.

22. Dickinson E, Davies E. Influence of ionic calcium on stability of sodium caseinate emulsions. Colloids and Surfaces B: Biointerfaces. 1999; 12: 203-212.

23. Liao W, Gharsallaoui A, Dumas E, Elaissari A. Understanding of the key factors influencing the properties of emulsions stabilized by sodium caseinate. Compr Rev Food Sci Food Saf. 2022; 21: 5291-5317.

24. Dickinson E. Strategies to control and inhibit the flocculation of protein-stabilized oil-in-water emulsions. Food Hydrocolloids. 2019; 96: 209-223.

25. Li M, O'Mahony JA, Kelly AL, Brodkorb A. The influence of temperature- and divalent-cation-mediated aggregation of β-casein on the physical and microstructural properties of β-casein-stabilised emulsions. Colloids Surf B Biointerfaces. 2020; 187: 110620.

26. Xi Y, Liu B, Jiang H, Yin S, Ngai T, Yang X. Sodium caseinate as a particulate emulsifier for making indefinitely recycled pH-responsive emulsions. Chem Sci. 2020; 11: 3797-3803.

27. Armand M, Pasquier B, André M, Borel P, Senft M, Peyrot, et al Digestion and absorption of 2 fat emulsions with different droplet sizes in the human digestive tract. Am J Clin Nutr. 1999; 70: 1096-1106.

28. Song H, Chai W, Yang F, Ren M, Chen F, Guan W, et al. Effects of Dietary Monoglyceride and Diglyceride Supplementation on the Performance, Milk Composition, and Immune Status of Sows During Late Gestation and Lactation. Front Vet Sci. 2021; 8: 714068.

29. Franziska Böttger, Didier Dupont, Dorota Marcinkowska, Balazs Bajka, Alan Mackie, Adam Macierzanka. Which casein in sodium caseinate is most resistant to in vitro digestion? Effect of emulsification and enzymatic structuring. Food Hydrocolloids. 2019; 88: 114-118.

30. Somayeh Sabouri, Amanda J. Wright, Milena Corredig. In vitro digestion of sodium caseinate emulsions loaded with epigallocatechin gallate. Food Hydrocolloids. 2017; 69: 350-358.

31. Sarkar A, Zhang S, Holmes M, Ettelaie R. Colloidal aspects of digestion of Pickering emulsions: Experiments and theoretical models of lipid digestion kinetics. Adv Colloid Interface Sci. 2019; 263: 195-211.

32. Shuning Zhang, Brent S. Murray, Melvin Holmes, Rammile Ettelaie, Anwesha Sarkar. Gastrointestinal Fate and Fatty Acid Release of Pickering Emulsions Stabilized by Mixtures of Plant Protein Microgels + Cellulose Particles: An In Vitro Static Digestion Study. Food Biophysics. 2023; 18: 120-132.

33. Qazi MJ, Schlegel SJ, Backus EHG, Bonn M, Bonn D, Shahidzadeh N. Dynamic Surface Tension of Surfactants in the Presence of High Salt Concentrations. Langmuir. 2020; 36: 7956-7964.

34. C. Roldan-Cruz, E.J. Vernon-Carter, J. Alvarez-Ramirez. Assessing the stability of Tween 80-based O/W emulsions with cyclic voltammetry and electrical impedance spectroscopy. Colloids and Surfaces A: Physicochemical and Engineering Aspects. 2016; 511: 145-152.

35. Vinarov Z, Tcholakova S, Damyanova B, Atanasov Y, Denkov ND, Stoyanov SD, et al. Effects of emulsifier charge and concentration on pancreatic lipolysis: 2. Interplay of emulsifiers and biles. Langmuir. 2012; 28: 12140-12150.

36. C. Cano-Sarmiento, D. I. Téllez-Medina, R. Viveros-Contreras, M. Cornejo-Mazón, C. Y. Figueroa-Hernández, E. García-Armenta, et al. Zeta Potential of Food Matrices. Food Engineering Rev. 2018; 10: 113-138.

37. Witayaudom P, Klinkesorn U. Effect of surfactant concentration and solidification temperature on the characteristics and stability of nanostructured lipid carrier (NLC) prepared from rambutan (Nephelium lappaceum L.) kernel fat. J Colloid Interface Sci. 2017; 505: 1082-1092.

38. Zhao S, Wang Z, Wang X, Kong B, Liu Q, Xia X, et al. Characterization of Nanoemulsions Stabilized with Different Emulsifiers and Their Encapsulation Efficiency for Oregano Essential Oil: Tween 80, Soybean Protein Isolate, Tea Saponin, and Soy Lecithin. Foods. 2023; 12: 3183.

39. Cheng Li, Abid Naeem, Jiangwen Shen, Weiwei Zha, Qingyun Zeng, Peng Zhang, et al. Advances in the pharmaceutical research of curcumin for oral administration. Open Chem. 2023; 21.

40. Hartlieb KJ, Ferris DP, Holcroft JM, Kandela I, Stern CL, Nassar MS, et al. Encapsulation of Ibuprofen in CD-MOF and Related Bioavailability Studies. Mol Pharm. 2017; 14: 1831-1839.

41. Pan X, Junejo SA, Tan CP, Zhang B, Fu X, Huang Q. Effect of potassium salts on the structure of γ-cyclodextrin MOF and the encapsulation properties with thymol. J Sci Food Agric. 2022; 102: 6387-6396.

42. Barkat Ali Khan, Naveed Akhtar, Haji Muhammad Shoaib Khan, Khalid Waseem, Tariq Mahmood, Akhtar Rasul, et al. Basics of pharmaceutical emulsions: A review. Af J Pharmacy Pharmacol. 2011; 5: 2715-2725.

43. Liu Y, Wei ZC, Deng YY, Dong H, Zhang Y, Tang XJ, et al. Comparison of the Effects of Different Food-Grade Emulsifiers on the Properties and Stability of a Casein-Maltodextrin-Soybean Oil Compound Emulsion. Molecules. 2020; 25: 458.

44. Infantes-Garcia MR, Verkempinck SHE, Guevara-Zambrano JM, Andreoletti C, Hendrickx ME, Grauwet T. Enzymatic and chemical conversions taking place during in vitro gastric lipid digestion: The effect of emulsion droplet size behavior. Food Chem. 2020; 326: 126895.

45. Jorge Rodríguez-Martínez, María Jesús Sánchez-Martín, Oscar López-Patarroyo, Manuel Valiente. Novel cannabinoid release system: Encapsulation of a cannabidiol precursor into γ-cyclodextrin metal-organic frameworks. Journal of Drug Delivery Science and Technology. 2023; 79: 104085.

46. Si Y, Luo H, Zhang P, Zhang C, Li J, Jiang P, et al. CD-MOFs: From preparation to drug delivery and therapeutic application. Carbohydr Polym. 2024; 323: 121424.

47. Chen Y, Tai K, Ma P, Su J, Dong W, Gao Y, et al. Novel γ-cyclodextrin-metal-organic frameworks for encapsulation of curcumin with improved loading capacity, physicochemical stability and controlled release properties. Food Chem. 2021; 347: 128978.

48. Zhou Y, Zhang M, Wang C, Ren X, Guo T, Cao Z, et al. Solidification of volatile D-Limonene by cyclodextrin metal-organic framework for pulmonary delivery via dry powder inhalers: In vitro and in vivo evaluation. Int J Pharm. 2021; 606: 120825.

49. Feng L, Wang KY, Day GS, Ryder MR, Zhou HC. Destruction of Metal-Organic Frameworks: Positive and Negative Aspects of Stability and Lability. Chem Rev. 2020; 120: 13087-13133.

50. Ding, Xuechao Cai, Hai-Long Jiang. Improving MOF stability:

Approaches and applications. Chem Sci. 2019; 10: 10209-10230.

51. Sarah V. Dummert, Haneesh Saini, Mian Zahid Hussain, Khushboo Yadava, Kolleboyina Jayaramulu, Angela Casini, et al. Cyclodextrin metal–organic frameworks and derivatives: Recent developments and applications. Chem Society Rev. 2022; 51: 5175-5213.

52. Topuz F, Uyar T. Recent Advances in Cyclodextrin-Based Nanoscale Drug Delivery Systems. Wiley Interdiscip Rev Nanomed Nanobiotechnol. 2024; 16: e1995.

53. Lv M, Sun DW, Huang L, Pu H. Precision release systems of food bioactive compounds based on metal-organic frameworks: synthesis, mechanisms and recent applications. Crit Rev Food Sci Nutr. 2022; 62: 3991-4009.

54. Manousi N, Giannakoudakis DA, Rosenberg E, Zachariadis GA. Extraction of Metal Ions with Metal-Organic Frameworks. Molecules. 2019; 24: 4605.

55. Wang YH, Ke XM, Zhang CH, Yang RP. Absorption mechanism of three curcumin constituents through in situ intestinal perfusion method. Braz J Med Biol Res. 2017; 50: e6353.

56. Xue M, Cheng Y, Xu L, Zhang L. Study of the Intestinal Absorption Characteristics of Curcumin In Vivo and In Vitro. J Appl Pharmacy. 2017; 9: 1-6.

57. Hsieh YW, Huang CY, Yang SY, Peng YH, Yu CP, Chao PD, et al. Oral intake of curcumin markedly activated CYP 3A4: in vivo and ex-vivo studies. Sci Rep. 2014; 4: 6587.

58. Wortelboer HM, Usta M, van der Velde AE, Boersma MG, Spenkelink B, van Zanden JJ, et al. Interplay between MRP inhibition and metabolism of MRP inhibitors: the case of curcumin. Chem Res Toxicol. 2003; 16: 1642-1651.

59. Qianyu Ye, Sophie Kwon, Zi Gu, Cordelia Selomulya. Stable nanoemulsions for poorly soluble curcumin: From production to digestion response in vitro. J Mol Liquids. 2024; 394: 123720.

60. Zheng B, McClements DJ. Formulation of More Efficacious Curcumin Delivery Systems Using Colloid Science: Enhanced Solubility, Stability, and Bioavailability. Molecules. 2020; 25: 2791.

61. He Y, Hou X, Guo J, He Z, Guo T, Liu Y, et al. Activation of a gamma-cyclodextrin-based metal-organic framework using supercritical carbon dioxide for high-efficient delivery of honokiol. Carbohydr Polym. 2020; 235: 115935.

62. Menglu Li, Yinlin Shao, Shengling Tang, Le Zhang, Minghua Yang, Tingting Zhu, et al. Crosslinked γ-cyclodextrin metal organic framework for stable ibuprofen loading. Materials Res Express. 2023; 10: 105014.

63. Li X, Uehara S, Sawangrat K, Morishita M, Kusamori K, Katsumi H, et al. Improvement of intestinal absorption of curcumin by cyclodextrins and the mechanisms underlying absorption enhancement. Int J Pharm. 2018; 535: 340-349.

64. Nasr G, Greige-Gerges H, Fourmentin S, Elaissari A, Khreich N. Cyclodextrins permeabilize DPPC liposome membranes: a focus on cholesterol content, cyclodextrin type, and concentration. Beilstein J Org Chem. 2023; 19: 1570-1579.

65. Wang CM, Fernez MT, Woolston BM, Carrier RL. Native gastrointestinal mucus: Critical features and techniques for studying interactions with drugs, drug carriers, and bacteria. Adv Drug Deliv Rev. 2023; 200: 114966.

66. Chen L, Huang W, Hao M, Yang F, Shen H, Yu S, et al. Rapid and ultrasensitive activity detection of α-amylase based on γ-cyclodextrin crosslinked metal-organic framework nanozyme. Int J Biol Macromol. 2023; 242: 124881.

67. Yu H, Huang Q. Investigation of the absorption mechanism of solubilized curcumin using Caco-2 cell monolayers. J Agric Food Chem. 2011; 59: 9120-9126.